Journal of Catalysis **190,** 1–13 (2000)
doi:10.1006/jcat.1999.2744, available online at http://www.idealibrary.com on IDEAL®

A Temperature-Programmed-Reduction Study on Alkali-Promoted, Carbon-Supported Molybdenum Catalysts

Lijuan Feng,[1] Xianguo Li,[1] Dady B. Dadyburjor,[2] and Edwin L. Kugler

Department of Chemical Engineering, CEMR, P.O. Box 6102, West Virginia University, Morgantown, West Virginia 26506-6102

Received February 24, 1999; revised October 29, 1999; accepted October 29, 1999

The reducibility of a series of carbon-supported, molybdenum-based catalysts with or without a potassium promoter was investigated using temperature-programmed reduction (TPR). The Mo loading and the K-doping level influence the reducibility of the K-Mo/C catalysts. The TPR spectra of both Mo/C and K-promoted Mo/C catalysts generally consist of four peaks. Two of these (located around 350 and 440°C) are attributed to the reduction of octahedrally coordinated Mo [Mo(O)], and a third peak (located around 740°C) is attributed to the reduction of tetrahedrally coordinated Mo [Mo(T)]. The fourth peak (located around 850°C) is assigned to CO desorption from the decomposition of the oxidized carbon support. The distribution of the different Mo species is greatly affected by the Mo loading and the K-doping level. In the absence of the K promoter, Mo(O) species predominate at relatively low metal loadings while Mo(T) species predominate at higher loadings. The reducibility of both species, quantified by the hydrogen consumed, or the average Mo valence, decreases with increasing Mo loadings. The K/C runs indicate that K itself is not reduced, but it may modify the reducibility of other metal compounds. A small amount of K, when added to the Mo/C, increases the area of the low-temperature Mo(O) peaks at the expense of the high-temperature Mo(T) peak. Under these conditions, the Mo(T) is significantly more reduced than is the Mo(O). Larger amounts of K decrease the Mo(T) peak area and cause less reduction in both the Mo(T) and Mo(O) species. K and Mo interact in K-promoted Mo/C catalysts, with the interaction being most pronounced for molar ratios of K/Mo between 0.2 and 1.

Key Words: **TPR; molybdenum; activated carbon; potassium.**

INTRODUCTION

Molybdenum-based catalysts are active for many kinds of catalytic reactions, including hydrogenation, hydrogenolysis, hydrocracking, hydrodesulfurization, and hydrodenitrogenation. The catalytic performance depends, to a certain extent at least, on the support used, since the surface properties of the catalyst vary with the support. Alumina, silica, and silica–alumina are commonly used for hydrotreating and hydrocracking catalysts (1), and for the synthesis of hydrocarbons (2–5) and alcohols (6–8) from carbon oxides (monoxide or dioxide) and hydrogen. A carbon support has also been used for hydrocarbon synthesis (9) and for higher-alcohol synthesis (10–13). A carbon support possesses advantages over oxide supports for some reactions because of its inactive surface, which could lead to a weak interaction between the support and the active components, thus preferentially forming active phases and making them more effective (14). Further, specially pretreated carbon supports can prevent coke formation on the surface of catalyst so that the life of the catalyst increases (14, 15).

Both oxides and sulfides of molybdenum can be used as catalysts for the synthesis of mixed alcohols. Whether the molybdenum is originally in the oxide or sulfide form, the presence of alkali promoters and modifiers is essential for the formation of the mixed alcohols. Molybdenum-based catalysts promoted by potassium or cesium have been used for the synthesis of mixed alcohols from syngas (6–8, 10–13, 16–18), while unpromoted molybdenum catalysts produce mainly light hydrocarbons (9). The mechanism of the promotional effect of alkali still remains open to question. Some researchers (18) believe that the catalysts are bifunctional, while others (19) suggest that alkali atoms modify the local electron density of the transition metal, either directly or indirectly via the support. Generally, the nature, the doping level, and the counter-anion of the alkali affect the activity and selectivity of catalytic reactions (20–22).

Mo-based catalysts generally need to be reduced (6–8) or sulfided (10–13, 16–18) prior to reaction, in order to achieve the desired performance. The relative amount of different molybdenum species on the surface of the catalyst after the pretreatment dramatically affects the performance of the catalyst (23). Therefore, the reducibility of molybdenum-based catalysts is an interesting and important aspect for study. For this purpose, temperature-programmed reduction (TPR) is a useful technique (24).

[1] Current address: College of Chemistry and Chemical Engineering, Ocean University of Qingdao, Qingdao, Shandong 266003, People's Republic of China.

[2] To whom correspondence should be addressed. E-mail: dadyburjor@cemr.wvu.edu.

0021-9517/00 $35.00

It has been widely applied to oxide-supported Mo-based catalysts (25–27). For carbon-supported catalysts, at least one group (28) has investigated the reduction of molybdenum using thermogravimetry/mass-spectrometry (TG/MS). In the present work, we use TPR to study the reduction behavior of carbon-supported, molybdenum-based catalysts, both with and without a potassium promoter. In particular, we investigate the effects of molybdenum loading and potassium doping on the reducibility of the catalysts.

EXPERIMENTAL

Materials

Activated carbon was obtained from Aldrich Chemical Company. The granule size of the activated carbon is 20–40 mesh, the surface area is 660 m^2/g, and the pore volume is 1.0 ml/g. A sample of this carbon was sent to Galbraith Laboratories for elemental analysis. ICP results for metals present indicate 8.0% Si, 0.87% Al, 0.28% Fe, 0.18% Ca, 0.074% Mg, 0.069% Ba, smaller amounts of Sr and Ti, and measurable values in the ppm range of at least six other metals. The high concentration of silicon by elemental analysis is consistent with X-ray powder diffraction data which show strong lines for the cristobalite phase of SiO_2. Copper oxide (99.9999% CuO) and commercial molybdenum oxide (MoO_3) were also obtained from Aldrich Chemical Company. Ammonium heptamolybdate ($[NH_4]_6Mo_7O_{24}\cdot 4H_2O$) and potassium nitrate (KNO_3), used as the sources of molybdenum and potassium for catalyst preparation, were obtained from Fisher Scientific and were used as received. Gases argon (high purity, 99.995%) and a mixture of 10% hydrogen in argon were obtained from Matheson and used as received.

Catalyst Preparation

The incipient-wetness impregnation method was employed. The Mo/C samples were prepared by impregnating the activated carbon with an aqueous solution of ammonium heptamolybdate. This was followed by drying in air at 100°C overnight and then calcining in flowing N_2 at 500°C for 2 h. K/C samples were prepared by impregnating activated carbon with a solution of potassium nitrate, again followed by drying in air at 100°C overnight and calcining in flowing N_2 at 300°C for 2 h. For the Mo/C and K/C samples, loadings are given as the weight percent relative to the activated carbon support. The process used to prepare Mo-K/C catalysts was the same as that for the K/C samples, except that Mo/C was used in place of the activated carbon. For the Mo-K/C materials, nominal Mo percentages are based on the weight of activated carbon support, while potassium doping levels are given as the molar ratios of potassium to molybdenum.

Temperature-Programmed Reduction

The equipment used for temperature-programmed reduction was constructed from a Hewlett-Packard 5890 gas chromatograph and an external furnace with a temperature programmer. The sample to be analyzed was placed in a quartz U-tube reactor and surrounded with quartz chips. The reactor was heated using a furnace and temperature programmer obtained from Automated Test Systems (Butler, PA). Either high-purity Ar or the H_2-Ar mixture flowed through the reactor. The exit stream from the reactor passed through a cold trap filled with a mixture of dry ice and acetone (to remove water from the exit stream) and then to a thermal conductivity detector (TCD) in the gas chromatograph, where the H_2 content of the stream was monitored. A Hewlett-Packard personal computer and HP ChemStation Software were used for data acquisition and processing.

Approximately 120 mg of catalyst was used for each TPR experiment. The sample was first preheated in the high-purity Ar at 250°C for 1 h with a flow rate of 30 cc/min, to remove any absorbed volatile impurities. During this time, the reactor was isolated from the TCD, and separate streams flowed to the detection and reference arms of the TCD. Thus the TCD was uncontaminated by the exit stream from the reactor during pretreatment. The sample was then cooled down to room temperature in flowing Ar, and the TPR experiment was started. Typically, a TPR experiment was conducted in the H_2/Ar gas mixture flowing at 30 cc/min, the same flow rate used in the pretreatment. The temperature was usually ramped from room temperature to 850°C at a fixed rate of 10°C/min. The furnace was held at 850°C for 30 min. The H_2 consumption was monitored by the TCD. The TPR profiles of the samples were analyzed by deconvoluting them using PeakFit software from Jandel Scientific.

RESULTS

Reduction of CuO

In a calibration experiment, TPR data were collected using the high-purity CuO sample. This experiment was used to quantify the H_2 consumption during the reduction, and thus to calibrate the response of the TCD. The results allow us to obtain an average valence of Mo for the catalysts after reduction, assuming the initial oxidation state of the Mo to be +6.

Figure 1a shows the TPR spectrum of the CuO. Only one peak of H_2 consumption is observed. The peak is symmetric and occurs at a temperature of around 260°C. After the first TPR run, the sample was cooled to room temperature in flowing Ar, and a second TPR experiment was conducted, following exactly the same procedure as used in the first run. A very flat line was obtained (not shown in Fig. 1).

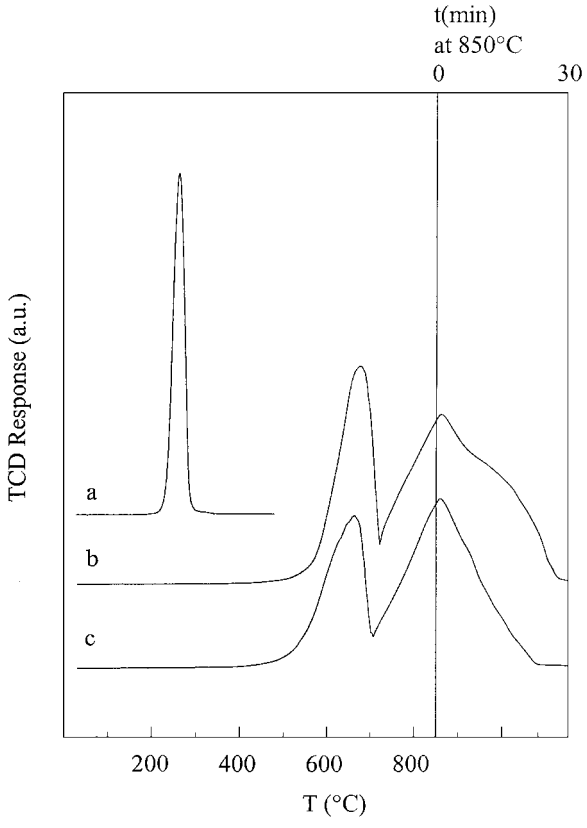

FIG. 1. TPR spectra when the sample is ramped from room temperature to 850°C, then held at 850°C for 30 min. Samples are as follows: (a) CuO; (b) commercial MoO_3; (c) in-house MoO_3.

In other words, no more H_2 was consumed in this second run. This indicates that CuO can be completely reduced at a relative low temperature in a single step. This experiment was readily repeatable. Therefore, the TCD response may be reliably calibrated by assuming stoichiometric reduction of the CuO.

Reduction of Unsupported Molybdenum Oxides

Figure 1b shows the TPR spectrum from the commercially obtained MoO_3, and Fig. 1c shows that from unsupported MoO_3 made in-house by calcining ammonium heptamolybdate in flowing N_2 at 500°C for 2 h. The TPR profiles of both the purchased MoO_3 and the prepared MoO_3 show two peaks of H_2 consumption: one at a temperature around 660°C, and the other at 850°C. The shape and location of the two peaks are very similar for the two samples. This suggests that the ammonium heptamolybdate is converted to MoO_3 after calcination in N_2 at 500°C.

TPR of Activated Carbon

The importance of blank runs using only the carbon support has been noted earlier (28). For the activated carbon, four experiments have been carried out. The first one was a TPR of the activated carbon. For the second run, a sample of activated carbon that had been calcined in flowing N_2 at 500°C for 2 h was used for the TPR experiment. After this second run, the same sample was cooled to room temperature in flowing Ar. The third run was also a TPR, but with the same sample used in run (b), without exposing the sample to air. In the final run, a fresh sample of activated carbon was calcined in N_2, like the sample used in run (b), and was then heated using pure Ar (rather than in a mixture of H_2 and Ar) following the same temperature program. In other words, this was a temperature-programmed desorption (TPD) run, rather than TPR. These four spectra are shown in Fig. 2.

Both the carbon sample (Fig. 2a) and the N_2-calcined carbon sample (Fig. 2b) exhibit a positive peak at a temperature around 570°C and a negative peak at around 850°C. Clearly, the N_2 calcination procedure has no significant effect on the TPR profile for the activated carbon. In the third run, where the TPR procedure was repeated for the same calcined carbon sample, only small fluctuations in the baseline are observed (Figs. 2c); there are no significant positive or negative peaks. Clearly, the reduction is complete after the first TPR run. In the TPD experiment without hydrogen

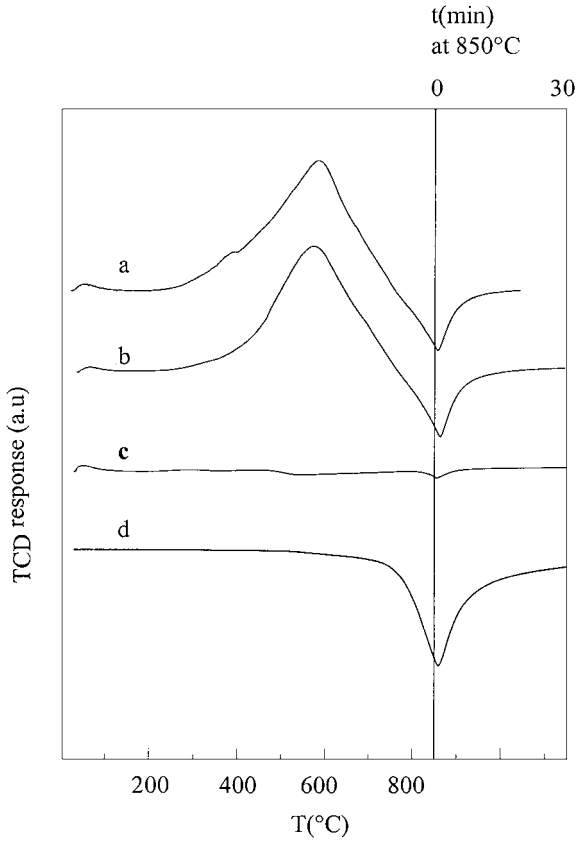

FIG. 2. Spectra for activated carbon support material: (a) TPR of fresh sample; (b) TPR of N_2-calcined sample; (c) repeated TPR of sample used for curve (b); (d) TPD of fresh sample.

(Fig. 2d), only one peak is obtained. This is the same negative peak observed in Figs. 2a and b. The presence of this peak even in the absence of hydrogen implies that the peak is unrelated to TPR. We return to this later.

The runs with CuO, unsupported Mo oxides, and the activated carbon support may be summarized as follows: the negative peak seen at 850°C is not relevant to TPR; the positive peaks observed correspond to hydrogen consumption due to reduction of the sample; and the reduction is complete after the first TPR experiment.

K/C Samples

The TPR profiles of K/C samples are presented in Fig. 3, curves b through e, with the TPR profile of the carbon support alone presented as curve a. Qualitatively, one positive peak, one shoulder, and one negative peak are observed for all the K/C samples. At low loadings of K (less than 6 wt%), the temperature position of the positive peak is nearly the same as that for the carbon support alone, and the impregnation of potassium makes the positive peak sharper. At the low loadings, a broad shoulder is observed at around 450°C, a temperature lower than the main (C-based) peak.

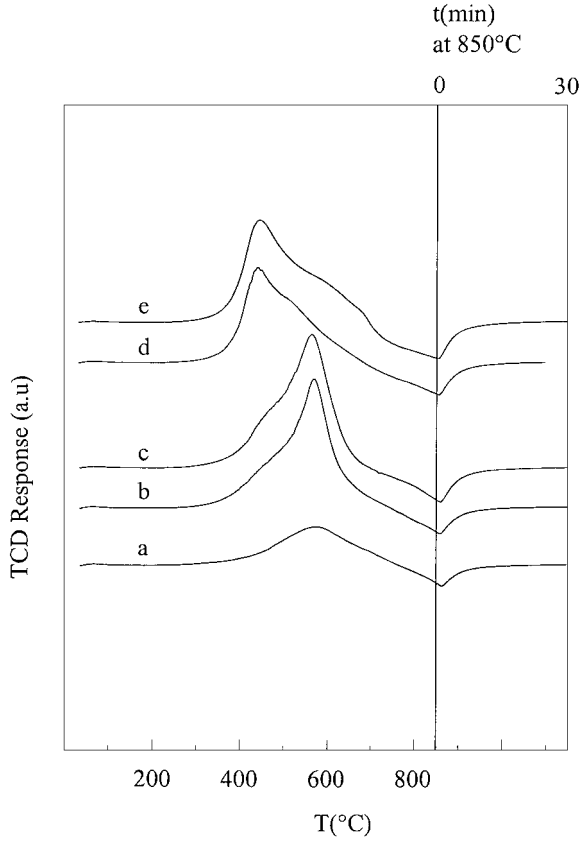

FIG. 3. TPR spectra for K/C samples. Loadings of K are as follows, in wt%, as weight of elemental K divided by weight of support: (a) 0; (b) 2.9; (c) 5.8; (d) 8.8; (e) 11.6.

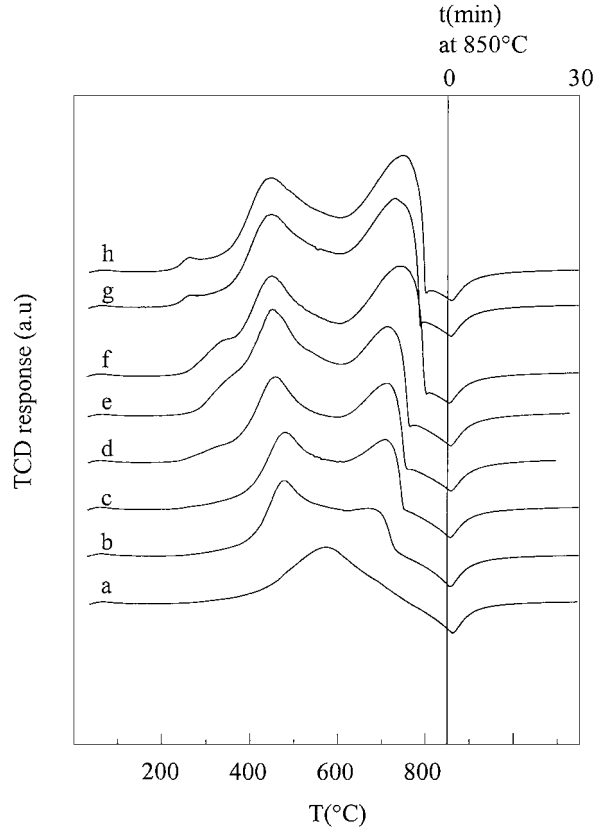

FIG. 4. TPR spectra for Mo/C samples. Loadings of Mo are as follows, in wt%, as weight of elemental Mo divided by weight of support: (a) 0; (b) 3; (c) 6; (d) 9; (e) 12; (f) 18; (g) 21; (h) 24.

When the potassium loading is relatively high (greater than 6 wt%), the broad shoulder narrows and is converted to a narrow peak, while the sharp main peak broadens into a shoulder. Further, the total area under the TPR spectrum, corresponding to the amount of H_2 consumed, increases significantly even when only 3 wt% K is added. However, addition of over 11 wt% K does not appear to increase the consumption of H_2 significantly beyond the initial increase.

These results imply that the potassium itself is not reduced but may influence the reduction of (impurities in) the carbon support. Further, the effect of K appears to change somewhere between loadings of 6 and 8 wt% K. Quantitative descriptions of the TPR peaks are given in the Discussion section.

Mo/C Catalysts

Figure 4 shows the TPR profiles of Mo/C catalysts with different Mo loadings. At 3% and 6% molybdenum loadings, curves b and c, three major peaks are observed. Two are positive peaks at temperatures around 440 and 720°C; the third is the negative peak at around 850°C, as observed in the TPD profile of the carbon support and determined to

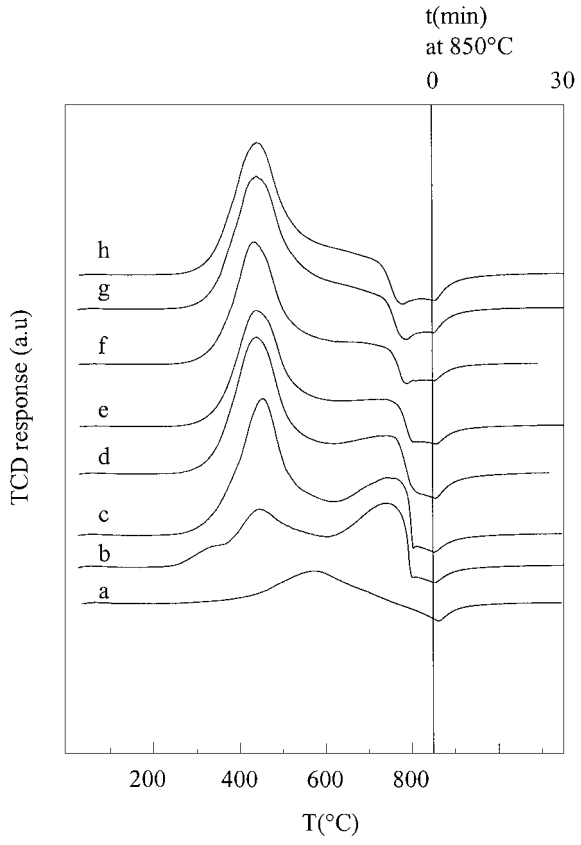

FIG. 5. TPR spectra for Mo-K/C catalysts. Curve (a), activated carbon support alone; for curves (b)–(h), Mo loadings are 18 wt% relative to the support, and K/Mo values are as follows, in molar ratio: (b) 0; (c) 0.2; (d) 0.6; (e) 1.0; (f) 1.2; (g) 1.4; (h) 1.6.

be irrelevant. On increasing the Mo loading to 9%, curve d, the position of the peak at around 720°C apparently shifts to a higher temperature, while that of the peak around 440°C moves slightly to a lower temperature. When the Mo loading reaches 9 wt%, a small shoulder develops near 300°C. The location of this fourth peak shifts to lower temperatures with increasing Mo loading. The areas of the peaks vary with Mo loading, with the higher-temperature peak accounting for a larger percentage of the total area as the loading increases. These peaks are quantitatively described in the Discussion section.

Mo-K/C Catalysts

Figure 5 gives the TPR profiles of Mo-K/C catalysts containing 18 wt% Mo with varying K-promotion level. Curve (a) is the TPR profile for the support alone, while curve (b) represents the TPR profile of the Mo/C catalyst without potassium, also shown in Fig. 4f. Qualitatively, at least three major peaks are seen for each catalyst: at least two positive peaks and one negative peak. This is analogous to the behavior of the Mo/C materials. Note that the peak at the lowest temperature (around 320°C) vanishes with the addition of even a small amount of K. Further, the presence of even the smallest loading of K dramatically alters the relative areas of the two major positive peaks. Increasing the K/Mo molar ratio from 0.2 to 1.6 does not cause much qualitative change in the TPR profiles, but the relative areas of the positive peaks do show small changes. Quantitative discussions of the TPR peaks are given below.

DISCUSSION

Unsupported Mo Oxide

Table 1 shows quantitative results from the TPR of the commercial MoO_3 and the MoO_3 prepared in-house, Fig. 1b and c. The locations of the low-temperature maximum (T_L) and the high-temperature maximum (T_H) are taken directly from the figure and are seen to be very close, but not identical, for the two materials. The small difference in the positions of the peaks might be caused by different amounts or different particle sizes of the MoO_3 used in the two experiments.

In Table 1, the hydrogen consumption entries (h) refer to the area of the corresponding peak, calibrated by TPR with CuO, assuming that the CuO is fully reduced to the metal. (As shown above, this is a reasonable assumption.) The Mo valence values (V_{Mo}) are calculated by assuming that the hydrogen is consumed by a stoichiometric reaction of the type

$$MoO_3 + hH_2 \rightarrow MoO_{(3-h)} + hH_2O, \qquad (1)$$

where h is the hydrogen consumption (mol H_2/mol MoO_3); the valence of Mo is then given by

$$V_{Mo} = 2(3 - h). \qquad (2)$$

According to Table 1, the ratio of the area of the high-temperature peak to the area of the low-temperature peak is approximately 3. Further, for both purchased and in-house MoO_3, the Mo valence value V_{Mo} after the low-temperature reduction (corresponding to the first peak) is close to +4, while $V_{Mo} \approx 0$ after the whole TPR run, i.e., metallic Mo is formed after the high-temperature reduction. These results suggest that the reduction of bulk MoO_3

TABLE 1

TPR Results of Unsupported MoO_3[a]

Sample	Location of maximum (°C)		H_2 consumption h (mol H_2/mol MoO_3)		Mo valence, V_{Mo}	
	T_L	T_H	L	H	L	H
Commercial	660	>850	1.07	3.13	3.86	−0.26
In-house	676	>850	1.04	3.10	3.92	−0.20

[a] L, low-temperature reduction; H, high-temperature reduction.

TABLE 2

TPR and TPD Curves for Activated Carbon Support

Experiment[a]	Location of maximum (°C)		Area (a.u.) × 10^{-6}	
	Positive peak	Negative peak	Positive peak	Negative peak
a	583	>850	6.76	1.04
b	573	>850	6.12	1.21
d	–	>850	–	3.76

[a] Letters correspond to curves of Fig. 2: (a) TPR of fresh sample; (b) TPR of N_2-calcined sample; (d) TPD of N_2-calcined sample.

under our TPR experimental conditions consists of two distinct steps. The MoO_3 is reduced to MoO_2 in the first step, while the MoO_2 is further reduced to metallic Mo at higher temperatures. This is consistent with literature data (29, 30).

Activated Carbon Support

For the activated carbon support, Table 2 lists the locations of the peaks as well as the integrated areas of the TPR curves and of the TPD curve, all based on Fig. 2. The parameters for the N_2-calcined samples and the fresh carbon samples are very similar to each other. This is an indication of the similarity of their reducibility.

Studies by Mims and co-workers (33, 34) have shown that graphite and glassy carbon surfaces are oxidized when exposed to air or water vapor. The oxidation occurs primarily on the edges rather than on the basal planes of graphite. The positive peak observed for the activated carbon support is most probably due to the reduction of the oxidized surface of the carbon. Alternatively, it is possible that some of the metal oxide impurities present in the activated carbon are reduced. While it is not clear as to which metal oxide might be responsible, an ICP analysis of impurities in the carbon support is reported in the Experimental section above.

For the negative peak, there are two major possibilities. The first possibility is the removal of gases from the carbon, gases having a higher thermal conductivity than that of the reducing gas (10% H_2 in Ar). The second possibility is the gasification of the carbon support, due to methanation in the H_2 atmosphere (31, 32). We show below that the latter possibility is unlikely; further, considerable experimental evidence in the literature points to the evolution of CO and CO_2 being responsible for the negative peak.

First, recall that the negative peak was also observed in the TPD experiment with the carbon support, i.e., in the absence of hydrogen, and the position of the negative peak is basically the same as that in the TPR curves, whether for the fresh carbon sample or for the N_2-calcined carbon sample. This rules out the possibility of methanation of the activated carbon as the source of the negative peak. Moreover, no distinguishable peak, positive or negative, was observed in the repeated TPR run, where the same calcined carbon sample was used after being cooled to room temperature following the first TPR run. This also shows that methanation of the carbon support is not important during TPR runs.

Further, Mims and co-workers (33, 34) found that CO is removed from the oxidized carbon surface (formed as noted above by exposure of the carbon to air or water vapor) when the substrate is heated in the temperature range 650–800°C in vacuum. In addition, Murchison and co-workers (28) showed that, in an inert atmosphere, the carbon support is significantly reduced to give off CO_2, while in a H_2/He mixture, reduction by H_2 predominates, with less than 2% reduction occurring via the carbon support. More recently, Otake and Jenkins (35) have comprehensively characterized four oxygen-containing functional groups on the surfaces of carbon, which are chemically and energetically different: surface complexes yielding CO at lower temperatures, and at high temperatures, and complexes yielding CO_2, again at lower temperatures and at high temperatures. The first two complexes evolve CO at maximum rates at 900 and 1100 K, respectively, and the remaining two evolve CO_2 at maximum rates at 600 and 900 K, respectively. Finally, Vannice and co-workers (36) have systematically compared the surface properties of different forms of carbon: activated carbon, graphitized carbon fibers, and synthetic diamond powder, with or without pretreatment. They found that comparable amounts of CO and CO_2 are desorbed for the untreated activated carbon sample, but that treatment with nitric acid results in evolution of carbon oxides in amounts almost an order of magnitude higher, while high-temperature treatment with H_2 leads to much smaller evolution of the gases, particularly CO. For the graphitized carbon fibers and diamond powder, more CO is desorbed than CO_2, but the total amount of carbon oxides desorbed is less than that corresponding to activated carbon.

The literature results noted clearly demonstrate that CO and CO_2 are given off when carbon, or carbon-supported catalysts, are subjected to heat in vacuum or in a nonoxidizing atmosphere. In our case, any CO or CO_2 released passes through the dry-ice/acetone trap. Since the thermal conductivities of CO and CO_2 are greater than that of argon, the thermal conductivity of the gas mixture increases. Therefore, it is likely that the negative peak in the TPR or TPD spectrum is produced by CO and CO_2 present in the gas phase because of the formation of oxides and their desorption from the activated carbon support.

The difference in the area of the negative peak between the TPD spectrum and the TPR spectrum can be attributed to two causes. First, differences in thermal conductivity for the Ar and H_2/Ar gas streams will produce different responses for a fixed amount of CO or CO_2. Hence, the same

response would not be expected in TPD and TPR experiments, even if the amount of CO or CO_2 desorbed were the same. Second, in the TPR experiment, some of the oxygen on the support reacts with H_2 at lower temperatures, giving positive peaks. Less oxygen remains at higher temperatures for activated carbon decomposition to form CO or CO_2. Hence, less CO or CO_2 should be produced in a TPR experiment.

K/C Samples

The TPR spectra for the K/C samples were shown in Fig. 3. It is reasonable to deconvolute these spectra into two positive peaks. One deconvolution for the 2.9% K sample is is shown in Fig. 6. Note that only positive peaks have been fitted. The spectrum appears to be fitted well using a Gaussian-type function. The two peaks are denoted as R (at 494°C) and S (at 570°C). These two peaks indicate that there are two reducible species in a K/C sample.

The location and area for each peak are summarized in Fig. 7 as a function of the amount of K present. The areas of peaks R and S change with the loading of K, but in a more-or-less complementary fashion—peak R decreases with increasing K, while peak S increases, so that the total area of the two peaks is nearly constant over the entire range of K loadings. That implies that K itself cannot be reduced under our experimental conditions for TPR. Kelemen and Mims (34, 37) drew similar conclusions from UPS measurements studying KOH adsorbed on graphite surfaces.

From Fig. 3, the total peak area is considerably greater than the area obtained for the carbon support alone. Further, peak S is fairly close to the peak for the carbon support alone. Hence, peak S is most probably from the reduction of the oxidized surface of the carbon support and/or the reduction of its impurity metal oxides, as justified above. The addition of (even a small amount of) K probably modifies the reducibilities of other metal oxides in the carbon support considerably. Hence, it is possible that peak R is from the reduction of a (second) impurity oxide in the carbon support, made more reducible by the presence of K.

Finally, Fig. 7 shows that the positions of both peak R and peak S shift to lower temperatures with increasing K-doping level. Hence the higher the K-doping level, the easier is the reduction of the two reducible species.

Mo/C Samples

Figure 8 shows the typical fitting result of a TPR profile for a Mo/C catalyst. Again, only positive peaks have been fitted, and a Gaussian-type function can be used. For the Mo/C samples, a closer examination of the TPR curves shows that the profiles can be generally deconvoluted into

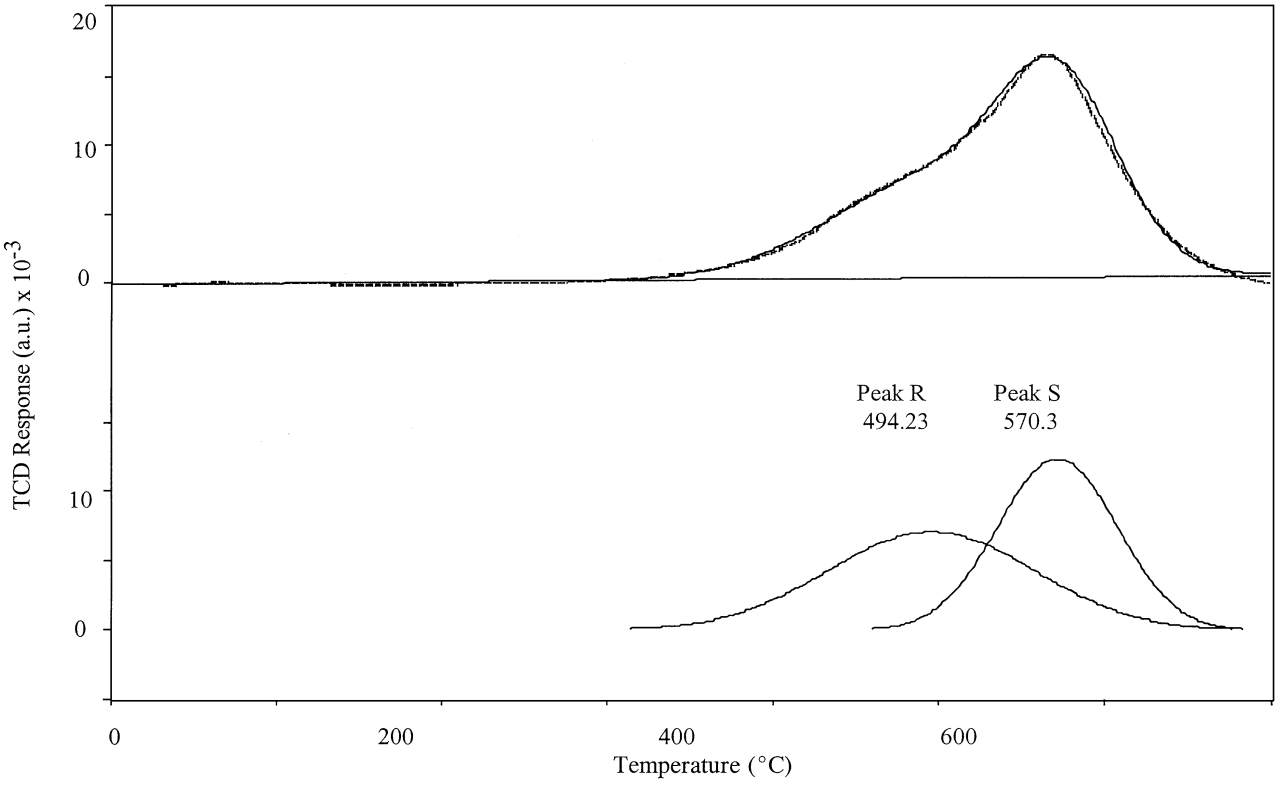

FIG. 6. Analysis of TPR spectrum for K/C sample (K loading = 5.8 wt%). Top, experimental curve and composite curve from analysis. Bottom, individual peaks from analysis.

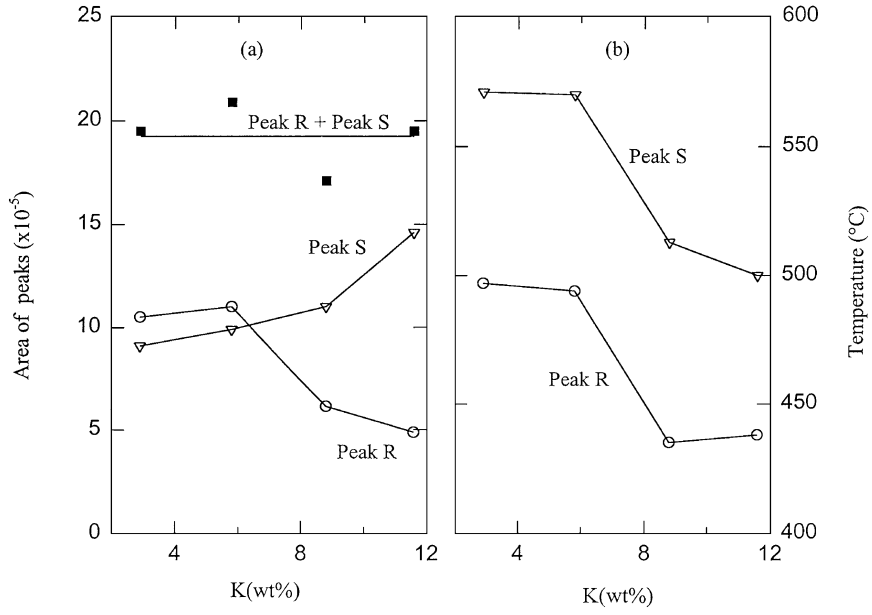

FIG. 7. Quantitative results from TPR of K/C samples as functions of K loading: (a) peak areas; (b) peak positions. Peak nomenclature as in Fig. 6.

four positive peaks, not three as qualitatively estimated earlier. (At Mo loadings above 9 wt%, an additional low-temperature peak may be observed. This is not considered here, as the magnitude of the corresponding area can be seen to be very small.) Of the four peaks, the next-to-highest, denoted as peak S, is again most probably from the reduction of the oxidized surface of the carbon support itself, and/or the reduction of its impurity metal oxides, as that peak is also shown in the case of the carbon support alone. The other three peaks are designated as X, Y, and Z as shown. Even though peak Y is close to the position of peak R in Figs. 6 and 7, peak Y is not ascribed to incremental reduction of an impurity by the presence of Mo. This is because Mo has not been reported to improve the reducibility of other species; we return to this later. Instead, peak Y, as well as peaks X and Z, correspond to the reduction of different Mo species on the carbon support. Peaks X and Y (which occur below peak S) are grouped together as

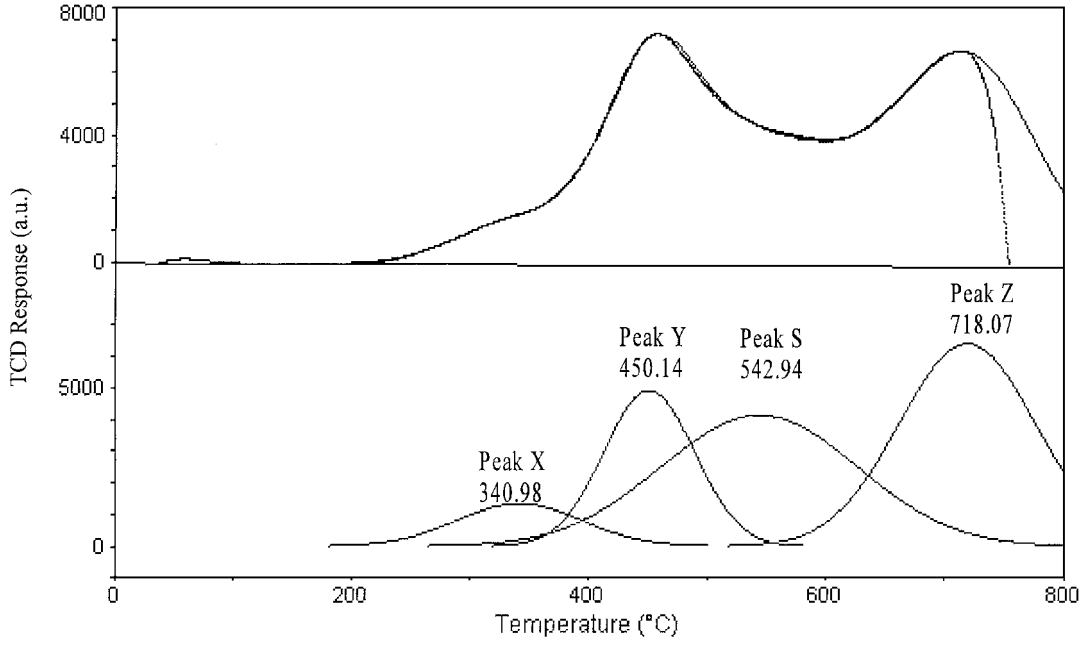

FIG. 8. Analysis of TPR spectrum for Mo/C sample (Mo loading = 9 wt%). (Top) Experimental curve and composite curve from analysis. (Bottom) Individual peaks from analysis.

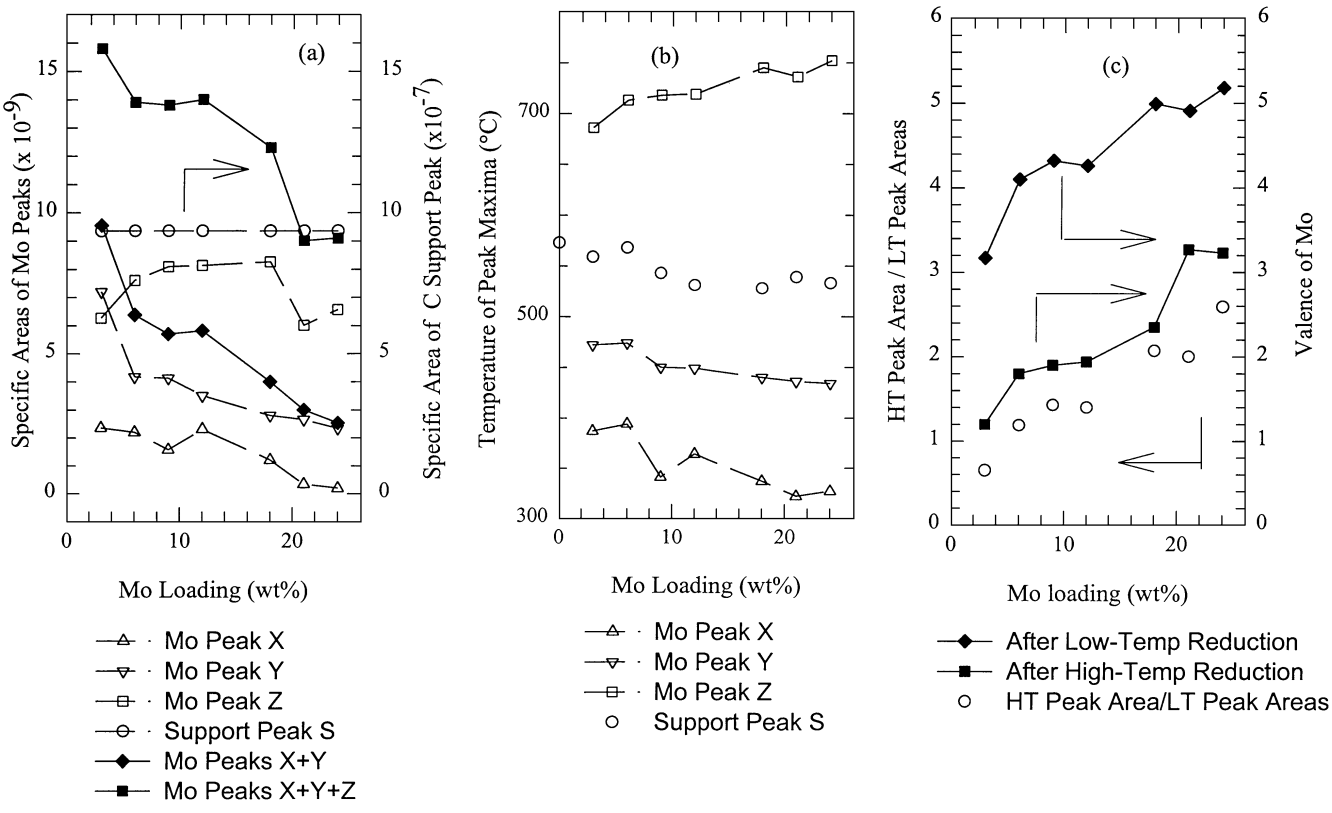

FIG. 9. Quantitative results from TPR of Mo/C samples as functions of Mo loading: (a) peak areas; (b) peak positions; (c) after-reduction valences of Mo and peak area ratio. Peak nomenclature as in Fig. 8.

low-temperature peaks, with peak Z (which occurs above peak S) being the high-temperature peak.

The positions and areas of the deconvoluted peaks are shown in Figs. 9a and b as functions of Mo loading. In performing the deconvolution, the reducibility of the impurities in the carbon support was assumed to remain unchanged when Mo is impregnated. In other words, the "specific" area of peak S, i.e., the area per mole of carbon in the samples, was constrained to stay the same during the deconvolution of all the samples, as shown in Fig. 9. However, the location of peak S, as given by the temperature corresponding to the maximum point of the peak, was allowed to change during the deconvolution procedure. The location of the peak is found to decrease with increased Mo loading, consistent with the behavior observed in Fig. 7.

We define specific areas of peaks X, Y, and Z on the basis of the moles of Mo in the sample. The specific areas of peaks X and Y decrease monotonically with Mo loading. The positions of these two peaks also decrease monotonically with loading. However, the specific area of peak Z passes through a maximum within the Mo loading range studied, and the location of peak Z shifts to higher temperatures with increasing Mo loading.

It should be noted that, while the specific area of peak Y decreases somewhat with Mo loading, the actual area of this peak increases. This is in contrast to the behavior of peak R in Fig. 7; the peak stays constant or decreases with K loading. Clearly, any reduction of support impurity that occurs in this region of the TPR spectrum of Mo/C is negligible, and all of peak Y may reasonably be ascribed to the reduction of an Mo species.

Shown in Fig. 9c are the calculated values of Mo valences after low- and high-temperature reductions. In both cases, the Mo valences increase with Mo loading. This indicates that the extent of reduction decreases with Mo loading. Consistent with this, Fig. 9c also shows that the ratio of the area of the high-temperature peak (Z) to the total area of the two low-temperature peaks (X and Y) increases with Mo loading. (This is also qualitatively noted in the Results.) Accordingly, varying the Mo loading changes not only the total amount of Mo in the catalyst, but also the distribution of the different Mo species.

It is widely recognized that the distribution of Mo species on supported Mo-based catalysts is influenced by the preparation method of the catalyst, such as the nature of support employed, the Mo precursor, and the drying and calcination conditions. For example, after a Mo/Al_2O_3 catalyst was dried, Mo was found to be converted from an octahedral coordination [Mo(O)] in paramolybdate ion to a tetrahedral coordination [Mo(T)]. Mo(T) was attributed to

$Al_2(MoO_4)_3$, either as a surface complex or as a bulk phase, whereas Mo(O) has been assigned to a surface complex such as $Al_2(Mo_7O_{24})$ or to bulk MoO_3. Upon calcination, both Mo(O) and Mo(T) species exist (1). Mo(T) and Mo(O) species have also been found in SiO_2-supported Mo catalysts (38).

A lower-temperature reduction peak in the TPR profiles has normally been assigned to the partial reduction of Mo and the reduction of readily reducible Mo species such as Mo(O), while a higher-temperature reduction peak has usually been attributed to the deep reduction of Mo, and the reduction of refractory Mo species such as Mo(T) (39). Hence, for our Mo/C samples, peak Z might arise because of the deep reduction of Mo species and/or the reduction of refractory Mo(T) species on the carbon support, while peaks Y and X may correspond to the partial reduction of Mo and/or the reduction of readily reducible Mo(O) species on the support.

The Mo(O) and Mo(T) species behave differently on the activated carbon support, in the present case, than has been reported for these materials on Al_2O_3 or SiO_2 supports. On Al_2O_3 or SiO_2 supports (38, 40, 41), the Mo(T) species (or the more-refractory Mo species) is dominant when the Mo loading is relatively low, but decreases in significance at higher loadings. However, for our Mo/C catalysts, the ratio of the area of the high-temperature peak to the total area of the two low-temperature peaks is greater than 1 only at a Mo loading of greater than 4–6 wt%; see Fig. 9c. In other words, the Mo(O) species predominates only at loadings of less than 4 wt%: at loadings of greater than 6 wt%, the amount of Mo(T) species on activated carbon is more than the amount of Mo(O) species.

Further, consider the effect of the support on low-temperature reductions as a function of metal loading. For Al_2O_3- and SiO_2-supported Mo-based catalysts, Rajagopal *et al.* (38) found that, when the reduction temperature is programmed to no higher than 550°C, the extent of reduction of Mo increases with increasing Mo loading. However, for our Mo/C catalysts at low temperatures, the extent of reduction of Mo decreases with Mo loading, and the Mo valence increases, as indicated by Fig. 9c.

Differences between the activated-carbon support and alumina or silica supports are observed also during the high-temperature reduction. For Mo/Al_2O_3 and Mo/SiO_2 catalysts, when the temperature of a TPR experiment was ramped to 900°C, the Mo was found to be almost completely reduced to the metal (38). In the present work, although complete reductions of unsupported MoO_3, both commercial and in-house, were achieved at high temperature, complete reduction of Mo was not observed for the supported Mo/C catalysts even at 850°C, the highest temperature used here. Further, for Mo/C, the extent of reduction of Mo after high-temperature reduction decreases with Mo loading. This trend, too, is completely different from that observed on Mo/Al_2O_3 and Mo/SiO_2 catalysts. Consistent with these observations, the increase in the ratio of the area of the high-temperature peak to the total area of the two low-temperature peaks with Mo loading is also totally different from that for Mo/Al_2O_3 and Mo/SiO_2 catalysts. For the latter catalysts, the ratio of Mo(T) (or Mo species reducible only at high temperature) to Mo(O) (or low-temperature reducible Mo species) decreases with Mo loading.

The reasons for these differences may be related to the surface properties of the support used. Note that the surface of Al_2O_3 contains mostly basic -OH groups, but it also contains some neutral -OH groups and some weakly acidic -OH groups (42, 43). The basic -OH groups are expected to react preferentially with MoO_4^{2-} ions, where the Mo coordination is tetrahedral, while the neutral or weakly acidic -OH groups react with $Mo_7O_{24}^{6-}$, where the Mo coordination is octahedral (1, 42–44). On alumina, for low Mo loading, much of the adsorbed Mo species retains tetrahedral coordination in a highly dispersed state, even after calcination. With increasing Mo loading, the interaction between Mo and the support becomes weaker, because of a decreased dispersion, thus leading to a smaller fraction of Mo(T) species upon drying and calcination. Heptamolybdate ions, attached to neutral or slightly acidic -OH groups, probably do not retain their identity upon calcination. Instead, they form multilayers of Mo oxide, in which Mo is believed to be present as Mo(O). Consistent with the isoelectric point of SiO_2 being lower than that of Al_2O_3, neutral and weakly acidic -OH groups are the major groups on the surface of SiO_2. That leads to a smaller fraction of the Mo species being present as Mo(T) on a SiO_2-supported catalyst than on an Al_2O_3-supported catalyst. This was confirmed by Rajagopal *et al.* (38). When activated carbon is used as the support, as in our case, the almost-inert surface of the carbon support could give rise to very weak interactions between the support and Mo. Therefore, upon calcination, multilayers of Mo oxide are expected to be formed predominantly, even at relatively low Mo loadings. For low-temperature reduction of C-supported catalysts, therefore, the extent of Mo reduction is deeper than when using Al_2O_3, or even SiO_2, as the support.

Mo-K/C Catalysts

We have shown earlier that K itself cannot be reduced under our experimental conditions; K as a promoter modifies the reducibilities of other compounds in the catalyst. Therefore, similar to those for Mo/C catalysts, the TPR spectra for Mo-K/C catalysts are also deconvoluted into four peaks. Figure 10 illustrates a typical TPR spectrum and the deconvoluted peaks for a Mo-K/C catalyst. The designation and the definition of those peaks are as in the case of the Mo/C samples. The results from the fitted TPR data are collected in Fig. 11, as a function of the K-doping level, quantified as the molar ratio K/Mo.

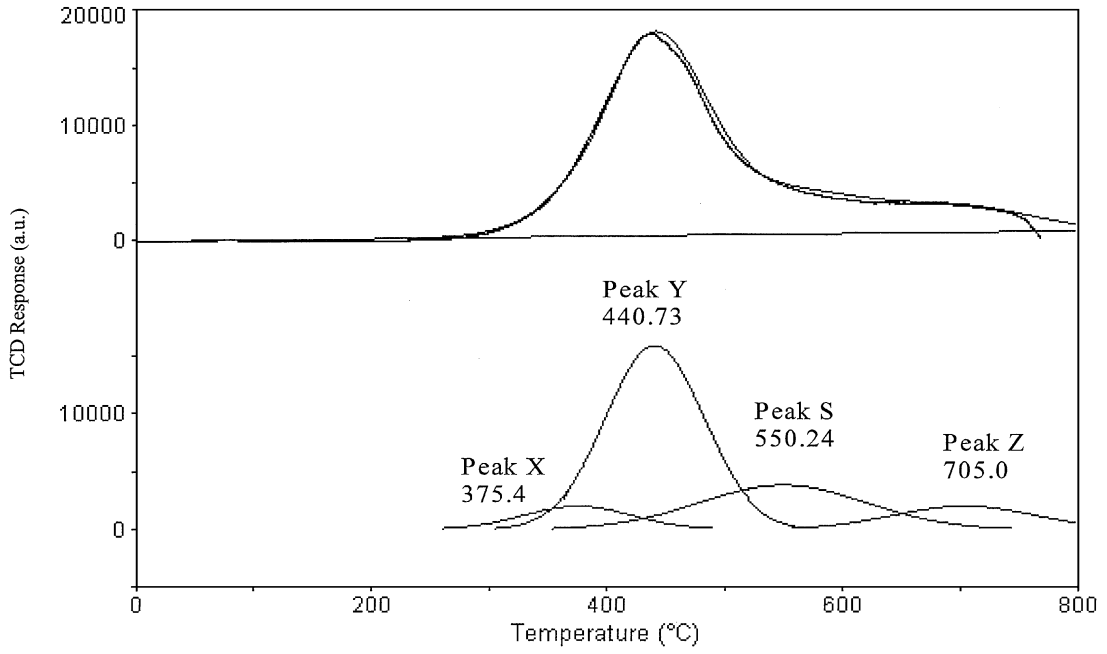

FIG. 10. Analysis of TPR spectrum for Mo-K/C sample (Mo loading = 18 wt%, K/Mo = 1.2). (Top) Experimental curve and composite curve from analysis. (Bottom) Individual peaks from analysis.

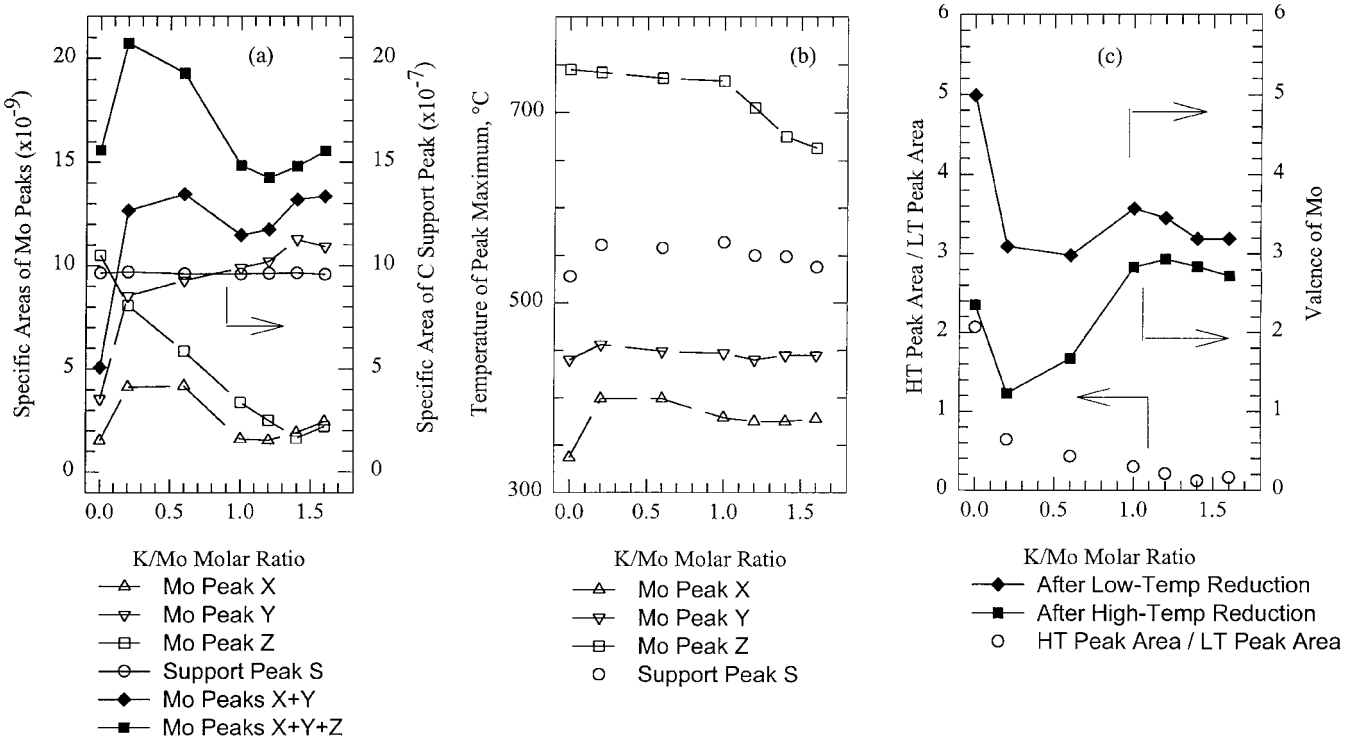

FIG. 11. Quantitative results from TPR of Mo-K/C samples with 18 wt% Mo loading as functions of K/Mo: (a) peak areas; (b) peak positions; (c) after-reduction valences of Mo and peak area ratio. Peak nomenclature as in Fig. 10.

As in Fig. 9, the specific area of peak S, i.e., the area per mole of carbon in the samples, was constrained to stay the same during the deconvolution of all the samples, while the location of peak S, as given by the temperature corresponding to the maximum point of the peak, was allowed to fluctuate. In this case, however, the location of peak S does not change with increasing K/Mo. For both the low-temperature peaks, X and Y, the specific areas, i.e., the areas per mole of Mo, increase greatly upon the addition of a small amount of K (K/Mo = 0.2); correspondingly, the specific area of the high-temperature peak, peak Z, decreases. With an increase in K/Mo, the specific area of peak X decreases, with a small local minimum around K/Mo = 1.2. Correspondingly, the specific area of peak Y continues to increase, but to a much smaller extent, with an increase in K/Mo. The total area of the low-temperature peaks, (X + Y), increases initially, then passes through a small local minimum around K/Mo = 1. On the other hand, the specific area of the high-temperature peak (peak Z) decreases monotonically with increasing K/Mo. The change of the total specific areas of the three positive peaks passes through a maximum around K/Mo = 0.4, with a local minimum around K/Mo = 1.2.

These results indicate that the initial addition of K greatly promotes the formation of a Mo species reducible at low-temperature (a Mo(O) species) and retards the generation of Mo species that are reducible only at high temperature (Mo(T) or other difficult-to-reduce Mo species). This means that Mo can be more easily reduced at low temperatures for catalysts with K than for those without K.

This trend can also be observed from the changes in the calculated Mo valences after low- and high-temperature reduction with increasing K/Mo values. The valence after low-temperature reduction decreases drastically with increasing K/Mo at low K/Mo values, then appears to level off around K/Mo = 1.4. The valence after high-temperature reduction also decreases rapidly at low K/Mo values, but then increases, again leveling off around K/Mo = 1. Similar to Mo/C catalysts, complete reduction of Mo was not observed for Mo-K/C catalysts under our TPR conditions.

The effects of the K promoter on the properties of unsupported or supported Mo-based catalysts have been investigated by many researchers. Xie and co-workers (20) verified that a new phase, consisting of K, S, Mo, and O, is formed on the surface of K_2CO_3-doped MoS_2 catalysts, and this phase enhances the performance of catalysts for the synthesis of higher alcohols (ethanols and higher). The amount of the new phase increases with increasing K concentration until the weight ratio K_2CO_3/MoS_2 reaches 0.6, corresponding to a K/Mo molar ratio of about 1.4. Jiang *et al.* (45) also confirmed the formation of a K–Mo interacting species, this one originating from the interaction between a KCl promoter and an alumina-supported molybdenum catalyst. In the case of Jiang *et al.*, the amount of the interacting species is saturated at a K/Mo molar ratio of 0.8. Jiang *et al.* also claimed that the formation of Mo(T) species is greatly suppressed by the addition of potassium.

Analogously, a new species could also be formed on the surface of the Mo-K/C catalysts considered in the present work, due to the interaction between the K promoter and the Mo component. The effect of the formation of the new phase on the reducibility of the Mo-K/C catalyst may be quantified by the changes in the average Mo valence. After both high- and low-temperature reductions, these changes are most pronounced for the initial addition of K, while saturation occurs at a K/Mo molar ratio of 1.0–1.4 in our case. This threshold value at which saturation is achieved probably depends on the potassium salt, the support, and other catalyst-preparation variables.

It should be noted that the addition of K does not always enhance the reduction of Mo at low-temperature; some literature references note the contrary. Tatsumi *et al.* (46) reported that K inhibits the reduction of Mo(VI) on K-Mo/SiO_2 catalysts. DeCanio *et al.* (47) observed that the reduction of Mo(VI) is depressed by the K promoter in Mo/γ-Al_2O_3. The reason for these differences is not clear.

SUMMARY AND CONCLUSIONS

A series of Mo-K/C catalysts were evaluated by means of TPR, and the results can be compared to unsupported catalysts as well as to catalysts supported on silica or alumina. First, the loading of Mo was increased, from 0 to 24 wt% of the activated carbon support. Then, for a fixed value of the Mo loading (18 wt%), the amount of the K dopant was increased from zero to a value corresponding to a molar ratio K/Mo = 1.6. A few runs were carried out with K/C samples as well. The TPR data were obtained by ramping from room temperature to 850°C at 10°C/min using a mixture of 10% H_2 in Ar at 30 cc/min.

For the Mo/C species, three major peaks were observed, in addition to a peak attributable to the reduction of the oxidized surface of the support and/or of impurities in the support. Of the three major peaks, the two peaks which are found at lower temperatures than the support peak are interpreted as being due to the reduction of Mo species with octahedral coordination, denoted as Mo(O). The third, high-temperature, peak is interpreted as being due to the reduction of tetrahedrally coordinated Mo, Mo(T). Analogous results have been reported in the literature for catalysts supported on alumina and on silica, except that generally only two peaks are observed. Contrary to what is found in Mo/Al_2O_3 and Mo/SiO_2 catalysts, Mo(O) species are predominant only at relatively low Mo loadings in the present case. Further, the reducibility of Mo decreases with increasing Mo loading. Finally, while unsupported Mo can be reduced to the zero-valent metal at high temperature, this is not possible for the C-supported material. The differences between the activated carbon support and alumina

or silica are probably because of the inert surface of the activated carbon.

The runs using K/C indicate that potassium itself cannot be reduced; as a promoter, K modifies the reducibility of the oxidized surface of the support or of other impurity oxide components present. The addition of a small amount of potassium to Mo/C increases the area of the low-temperature peaks and decreases the area of the high-temperature peak. Larger amounts of potassium decrease the high-temperature peak area but have correspondingly little effect on the low-temperature peaks. Hence the presence of K enhances the formation of low-temperature reducible Mo species, or octathedrally coordinated Mo(O), while retarding the generation of Mo species that are reducible only at high temperatures, or tetrahedrally coordinated Mo(T). At low values of the molar ratio K/Mo, the Mo after high-temperature reduction is significantly more reduced than after low-temperature reduction, as evidenced by the much lower value of the Mo valence for the high-temperature reduction. As the molar ratio K/Mo is increased, the Mo valence increases, but more so for the high-temperature reduction than for the low-temperature case. At a value of K/Mo around 1, the values of the Mo valence level off to approximately the same value for both high- and low-temperature reductions. The results are consistent with a K–Mo interacting species being formed at low K/Mo values, saturating at around K/Mo = 1. This is analogous to what has been observed in other cases.

ACKNOWLEDGMENT

We acknowledge the financial support from U.S. Department of Energy under Contract No. DE-AC22-91PC034.

REFERENCES

1. Massoth, F. E., *Adv. Catal.* **27**, 265 (1978).
2. Madon, R. J., Bucker, E. R., and Taylor, W. F., *Energy Res. Abstr.* **3**(14), Abstr. No. 32587 (1978).
3. Murchison, C. B., and Murdick, D. A., U.S. Patent 4,151,190 (1979).
4. Saito, M., and Anderson, R. B., *J. Catal.* **63**, 438 (1980).
5. Saito, M., and Anderson, R. B., *J. Catal.* **67**, 296 (1981).
6. Inoue, M., Miyake, T., Takegami, Y., and Inui, T., *Appl. Catal.* **29**, 285 (1987).
7. Tatsumi, T., Muramatsu, A., and Tominaga, H., *Appl. Catal.* **34**, 77 (1987).
8. Tatsumi, T., Muramatsu, A., and Tominaga, H., *Sekiyu Gakkaishi (J. Jpn. Petrol. Inst.)* **35**, 233 (1992).
9. Murchison, C. B., and Murdick, D. A., *Hydrocarbon Processing* **60**, 195 (1981).
10. Murchison, C. B., Conway, M. M., Stevens, R. R., and Quarderer, G. J., *in* "Proceedings, 9th International Congress on Catalysis, Calgary, 1988" (M. J. Phillips and M. Ternan, Eds.), p. 626. Chem. Institute of Canada, Ottawa, 1988.
11. Conway, M. M., Murchison, C. B., and Stevens, R. R., U.S. Patent 4,675,344 (1987).
12. Stevens, R. R., U.S. Patent 4,752,623 (1988).
13. Gunturu, A. K., Kugler, E. L., Cropley, J. B., and Dadyburjor, D. B., *Ind. Eng. Chem. Res.* **37**, 2107 (1998).
14. Duchet, J. C., van Oers, E. M., de Beer, V. H. J., and Prins, R., *J. Catal.* **80**, 386 (1983).
15. Laine, J., Severino, F., Labady, M., and Gallardo, J., *J. Catal.* **138**, 145 (1992).
16. Santiesteban, J. G., Bogan, C. E., Herman, R. G., and Klier, K., *in* "Proceedings 9th International Congress on Catalysis" (M. J. Phillips and M. Ternan, Eds.), p. 561. Chem. Institute of Canada, Ottawa, 1988.
17. Santiesteban, J. G., Ph.D. dissertation, Lehigh University, 1989.
18. Klier, K., Herman, R. G., Nunan, J. G., Smith, K. J., Bogdan, C. E., Yong, C.-W., and Santiesteban, J. G., *in* "Methane Conversion" (D. M. Bibby, C. D. Chang, R. F. Howe, and S. Yurchak, Eds.). Elsevier, Amsterdam, 1988.
19. Ailka, K., Hori, H., and Ozaki, A., *J. Catal.* **27**, 424 (1972).
20. Duan, L., Zhang, O., Ma, S., Li, S., and Xie, Y., *J. Mol. Catal. (China)* **4**, 208 (1990).
21. Fu, Y., Jiang, M., Bian, G., Du, Y., and Wei, J., *J. Mol. Catal. (China)* **21**, 27 (1993).
22. Lee, J. S., Kim, S., Lee, K. H., Nam, I.-S., Chung, J. S., Kim, Y. G., and Woo, H. C., *Appl. Catal. A* **110**, 11 (1994).
23. Yasumaru, J., Yamada, M., Houalla, M., and Hercules, D. M., *in* "Proceedings, 10th International Congress on Catalysis, Budapest, 1992" (L. Guczi, F. Solymosi, and P. Tentenyi, Eds.), p. 1867. Akadémiai Kiadò, Budapest, 1993.
24. Hurst, N. W., Gentry, S. J., Jones, A., and McNicol, B. D., *Catal. Rev.* **24**, 233 (1982).
25. Shimada, H., Sato, T., Yoshimura, Y., Hiraishi, J., and Nishijima, A., *J. Catal.* **110**, 275 (1988).
26. Valyon, J., Henker, M., and Wendlandt, K. P., *React. Kinet. Catal. Lett.* **38**, 265 (1989).
27. Thomas, R., van Oers, E. M., de Beer, V. H. J., Medema, J., and Moulijn, J. A., *J. Catal.* **76**, 241 (1982).
28. O'Connor, P. J., Whiting, L. F., and Murchison, C. B., *Thermochimica Acta* **127**, 1 (1988).
29. Arnoldy, P., de Jonge, J. C. M., and Moulijn, J. A., *J. Phys. Chem.* **89**, 4517 (1985).
30. Brito, J. L., Laine, J., and Pratt, K. C., *J. Mater. Sci.* **24**, 425 (1989).
31. Mims, C. A., and Krajewski, J. J., *J. Catal.* **102**, 140 (1986).
32. Mims, C. A., and Pabst, J. K., *J. Catal.* **107**, 209 (1987).
33. Kelemen, S. R., Freund, H., and Mims, C. A., *J. Vac. Sci. Technol. A* **2**, 987 (1984).
34. Kelemen, S. R., Freund, H., and Mims, C. A., *J. Catal.* **97**, 228 (1986).
35. Otake, Y., and Jenkins, R. G., *Carbon* **31**, 109 (1993).
36. Dandekar, A., Baker, R. T. K., and Vannice, M. A., *Carbon* **36**, 1821 (1998).
37. Kelemen, S. R., and Mims, C. A., *Surf. Sci.* **133**, 71 (1983).
38. Rajagopal, S., Marini, H. J., Marzari, J. A., and Miranda, R., *J. Catal.* **147**, 417 (1994).
39. Arnoldy, P., Franken, M. C., Scheffer, B., and Moulijn, J. A., *J. Catal.* **96**, 381 (1985).
40. Yao, H. C., *J. Catal.* **70**, 440 (1981).
41. Feng, L., Chen, S., and Peng, S., *Chem. J. Chin. Univ.* **16**(N1), 98 (1995).
42. van Veen, J. A. R., Hendriks, P. A. J. M., Romers, E. J. G. M., and Andrea, R. R., *J. Phys. Chem.* **94**, 5275 (1990).
43. Millman, W. S., Segawa, K., Smrz, D., and Hall, W. K., *Polyhedron* **5**, 169 (1986).
44. Ashley, J. H., and Mitchell, P. C. H., *J. Chem. Soc. A* 2730 (1969).
45. Jiang, M., Bian, G., and Fu, Y., *J. Catal.* **146**, 144 (1994).
46. Tatsumi, T., Muramatsu, A., and Tominaga, H., *J. Catal.* **101**, 553 (1986).
47. DeCanio, S. J., Cataloo, M. C., DeCanio, E. C., and Storm, D. A., *J. Catal.* **119**, 256 (1989).